

Monte Carlo Simulations of Liquid Acetic Acid and Methyl Acetate with the OPLS Potential Functions

James M. Briggs, Toan B. Nguyen, and William L. Jorgensen*

Department of Chemistry, Purdue University, West Lafayette, Indiana 47907 (Received: May 8, 1990)

Intermolecular potential functions have been developed for carboxylic acids and esters in the OPLS format by performing Monte Carlo simulations for liquid acetic acid at 25 and 100 °C and for liquid methyl acetate at 25 °C. The potential function parameters were chosen such that experimental thermodynamic and physical properties were reproduced within ca. 1–4%. In liquid acetic acid, the monomers are computed to be in an average of nearly two hydrogen bonds, there is a negligible occurrence of non-hydrogen-bonded monomers, and 7–16% of the monomers are in cyclic dimers. Some experimental studies have been interpreted to indicate that the liquid consists mostly of cyclic dimers, while others suggest that it is a mixture of linear and cyclic polymers, linear and cyclic dimers, and very few free monomers. In the current study it is found that liquid acetic acid consists mainly of hydrogen-bonded chains. Liquid methyl acetate is relatively structureless.

Introduction

Computer simulations can provide valuable energetic and structural information about chemical and biochemical systems.¹ A necessary component of these calculations is a description of the intermolecular interactions. To this end, optimized potentials for liquid simulations (OPLS) have been developed in our laboratory for water, hydrocarbons, common organic functional groups, peptides, and nucleotide bases.^{2–6} The development and testing of parameters for carboxylic acids and esters are presented here. A proper description of these functionalities is important since they provide common solvents and terminal groups for polypeptides, and they occur in the side chains of glutamic and aspartic acid. Though we have used the parameters for carboxylic acids and esters in prior studies,^{4,5a,7} detailed results on their development and performance in pure liquid simulations have not been provided. Consequently, results of Monte Carlo calculations for liquid acetic acid at 25 and 100 °C and for methyl acetate at 25 °C are presented here. The OPLS parameters were primarily fit to reproduce experimental data on the liquids through an iterative procedure using many simulations. The average structure of liquid acetic acid is also examined in detail, specifically with regard to the cyclic dimer content.

Computational Details

Monte Carlo Simulations. Statistical mechanics simulations were performed for liquid acetic acid and methyl acetate using the potential functions described in the following sections. Standard procedures were employed including Metropolis sampling and the isothermal-isobaric (NPT) ensemble.^{2–4} Each system consisted of 128 molecules in a cube of variable size with periodic boundary conditions. The calculations were performed at 1 atm and 25 or 100 °C. The normal boiling points are 117.9 °C for acetic acid and 56.9 °C for methyl acetate.⁸

The intermolecular interactions were spherically truncated at a distance of 12 Å based roughly on the centers-of-mass separation. A correction was made during the simulations for the Lennard-Jones interactions neglected beyond the cutoff; this lowers the total energy by 2–4% and has small effects as well on all other computed properties.³ A generally accepted procedure has not emerged to correct for the Coulombic interactions neglected beyond the cutoff. However, the lack of significant size dependence for many computed properties of liquid water should be noted.^{2b} New configurations were generated by randomly selecting a molecule, translating it randomly in all three Cartesian directions, rotating it randomly about a randomly chosen axis, and finally performing any appropriate internal rotations by a random amount. The translations and rotations were made within bounds of $\pm\Delta r$, $\pm\Delta\theta$, and $\pm\Delta\phi$, which were ± 0.15 Å, $\pm 15^\circ$, and $\pm 10^\circ$. Volume

TABLE I: Geometrical and OPLS Parameters for Acetic Acid and Methyl Acetate

Standard Geometrical Parameters ^a							
acetic acid				methyl acetate			
C=O	1.214	∠COH	107	C=O	1.200	∠COC	115
C–O	1.364	∠OCO	123	C–O	1.344	∠O=CC	125
CH ₃ –C	1.520	∠CC–O	111	CH ₃ –C	1.520	∠CC–O	110
O–H	0.970			CH ₃ –O	1.437		
OPLS Parameters							
atom or group	<i>q</i> , e	σ , Å	ϵ , kcal/mol				
Acetic Acid							
O	–0.58	3.00	0.170				
C	0.55	3.75	0.105				
=O	–0.50	2.96	0.210				
H	0.45	0.0	0.0				
CH ₃	0.08	3.91	0.160				
Methyl Acetate							
O	–0.40	3.00	0.170				
C	0.55	3.75	0.105				
=O	–0.45	2.96	0.210				
CH ₃ (–O)	0.25	3.80	0.170				
CH ₃ (–C)	0.05	3.91	0.160				

^a Bond lengths in angstroms, bond angles in degrees. Standard geometries are based on data summarized in ref 11.

changes were attempted every 700 configurations. This is performed by randomly selecting a volume change bounded by $\pm\Delta V$ (± 300 Å³) and then by scaling accordingly all of the intermolecular distances. The ranges designated above provided an acceptance rate for new configurations of ca. 40%.

(1) (a) McCammon, J. A.; Harvey, S. C. *Dynamics of Proteins and Nucleic Acids*; Cambridge University Press: Cambridge, 1987. (b) Jorgensen, W. L. *Acc. Chem. Res.* **1989**, *22*, 184.

(2) (a) Jorgensen, W. L.; Chandrasekhar, J.; Madura, J. D.; Impey, R. W.; Klein, M. L. *J. Chem. Phys.* **1983**, *79*, 926. (b) Jorgensen, W. L.; Madura, J. D. *Mol. Phys.* **1985**, *56*, 1381.

(3) Jorgensen, W. L.; Madura, J. D.; Swenson, C. J. *J. Am. Chem. Soc.* **1984**, *106*, 6638.

(4) Jorgensen, W. L.; Briggs, J. M.; Contreras, M. L. *J. Phys. Chem.* **1990**, *94*, 1683.

(5) (a) Jorgensen, W. L.; Tirado-Rives, J. *J. Am. Chem. Soc.* **1988**, *110*, 1657. (b) Jorgensen, W. L.; Swenson, C. J. *J. Am. Chem. Soc.* **1985**, *107*, 569. (c) Jorgensen, W. L. *J. Phys. Chem.* **1986**, *90*, 6379.

(6) Jorgensen, W. L.; Pranata, J. *J. Am. Chem. Soc.* **1990**, *112*, 2008.

(7) Jorgensen, W. L.; Boudon, S.; Nguyen, T. B. *J. Am. Chem. Soc.* **1989**, *111*, 755.

(8) Riddick, J. A.; Bunger, W. B.; Sakano, T. K. *Organic Solvents*, 4th ed.; Wiley-Interscience: New York, 1986; pp 361, 391.

* Address correspondence to this author at the Department of Chemistry, Yale University, New Haven, CT 06511.

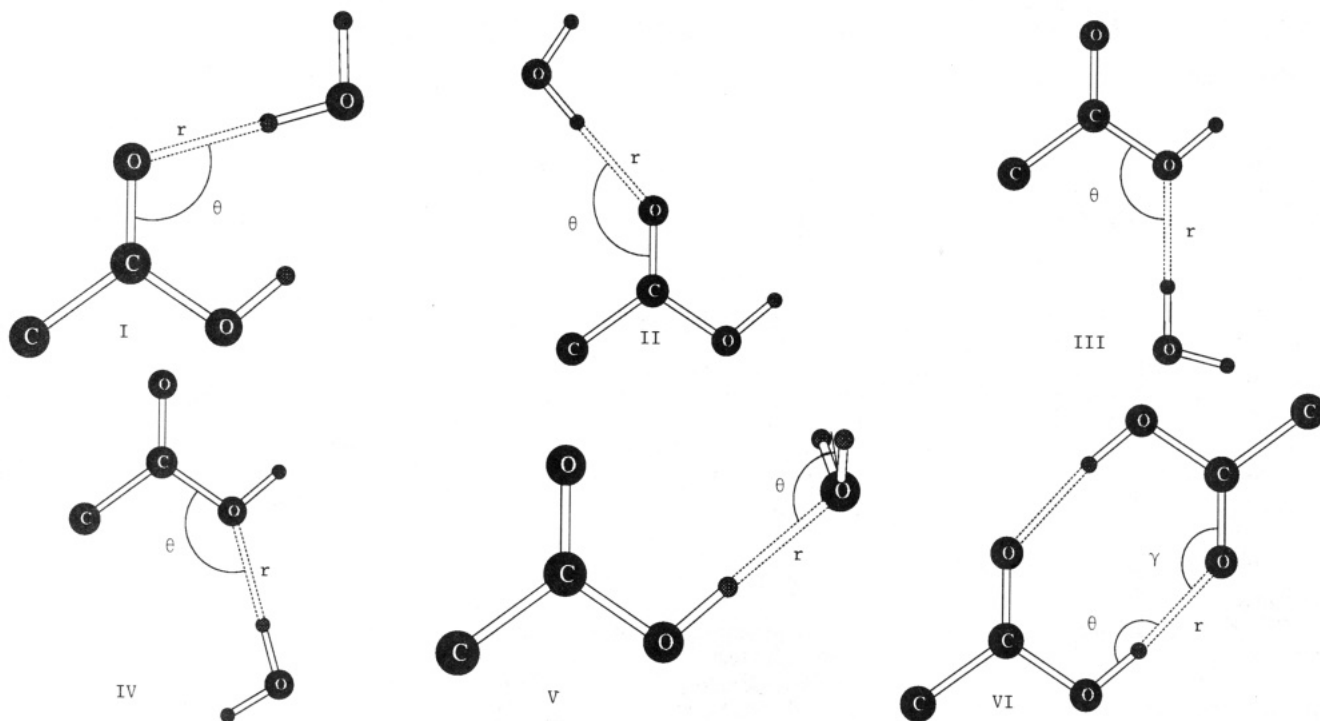


Figure 1. Geometrical arrangements for the five acetic acid-water complexes (I-V) and the cyclic dimer (VI). The four methyl acetate-water geometries are analogous to structures I-IV.

The simulation of methyl acetate was equilibrated for 400 K configurations and averaged for 1500 K. However, owing to the greater cohesiveness of acetic acid, 6000 K configurations were used for equilibration in this case followed by 2500 K of averaging. Initial configurations were derived from earlier simulations of liquid amides.^{5b} The calculations were performed mostly on Sun 4/260 and Silicon Graphics 4D/25S computers in our laboratory.

Intermolecular Potential Functions. The molecules are represented by interaction sites located on each nucleus with the exception that a united atom model is used for methyl groups that have a single site centered on the carbon. Hydrogen atoms attached to heteroatoms are represented explicitly.^{4,5} The total intermolecular energy of a dimer is defined as a double sum of Coulomb and Lennard-Jones interactions between all pairs of sites, *a* and *b*, on the two monomers (eq 1). Standard combining rules

$$\Delta E_{ab} = \sum_i \sum_j \left(q_i q_j e^2 / r_{ij} + A_{ij} / r_{ij}^{12} - C_{ij} / r_{ij}^6 \right) \quad (1)$$

are employed such that $A_{ij} = (A_{ii}A_{jj})^{1/2}$ and $C_{ij} = (C_{ii}C_{jj})^{1/2}$, where $A_{ii} = 4\epsilon_i\sigma_i^{12}$ and $C_{ii} = 4\epsilon_i\sigma_i^6$ in terms of Lennard-Jones σ 's and ϵ 's. Standard bond lengths and bond angles were used for the monomers and were held fixed throughout the simulations, as summarized in Table I. The OPLS parameters were developed by considering results discussed below for gas-phase complexes and by requiring that they reproduce experimental thermochemical and structural information on the liquids.

The number of new parameters was kept to a minimum by using parameters from related molecules to a large extent. The Lennard-Jones parameters for methyl acetate and acetic acid were taken entirely from earlier work on ethers⁹ and amides.^{5b} These parameters for the hydroxy and alkoxy oxygens were adopted from ether oxygens, while the parameters for the carbonyl groups and the methyl groups were taken from the work on amides. Lennard-Jones parameters for the acid hydrogen were assigned to be zero consistent with the practice for hydrogens on heteroatoms in amides, water, alcohols, and thiols.^{2,4,5} Initial charges were obtained from Mulliken population analyses of 6-31G(d) wave functions for the molecules in their experimental geometries as

well as from earlier work on *N*-methylacetamide.^{5b} The charges were then adjusted to give reasonable results for bimolecular complexes and for the pure liquids. The final charges, as listed in Table I, give dipole moments of 1.44 and 1.51 D for *Z*-methyl acetate and *Z*-acetic acid. The experimental values are 1.72 and 1.74 D.¹⁰

Internal Rotation. Torsional motion about the central C-O bond in methyl acetate and acetic acid was included in the simulations. The rotational potential is represented by the Fourier series in eq 2. As in previous work,³ the function was fit to results

$$V(\Phi) = \frac{1}{2}V_1(1 + \cos \Phi) + \frac{1}{2}V_2(1 - \cos 2\Phi) \quad (2)$$

of MM2 calculations.¹¹ The CCOR dihedral angle is taken as Φ , so the global minima are at 180° for the *Z* conformers. Few related experimental data exist for acetic acid and its methyl ester; however, there are more data for formic acid and methyl formate. Microwave studies put the barrier height to rotation about the C-O bond in formic acid at 13.8¹² and 17.0 kcal/mol,¹³ while IR work gave 10.0,¹⁴ 10.9,¹⁵ and 13.4 kcal/mol.¹⁶ Raman and neutron diffraction experiments yielded *E/Z* energy differences of 3.90¹⁷ and 4.78 kcal/mol.¹⁸ Furthermore, IR studies put the barrier to rotation in methyl formate at 10.0 kcal/mol¹⁴ and the *E/Z* energy difference at 3.85 and 4.75 kcal/mol.¹⁹

For acetic acid and methyl acetate, barrier heights of 10 and 15 kcal/mol were obtained from an IR study.¹⁴ The corresponding barrier heights from MM2 calculations are 8.92 and 9.26 kcal/mol

(10) Weast, R. C., Ed. *CRC Handbook of Chemistry and Physics*; CRC Press: Boca Raton, FL, 1988; pp E55-58.

(11) Allinger, N. L.; Chang, S. H.-M. *Tetrahedron* **1977**, *33*, 1561.

(12) Bjarnov, E.; Hocking, W. H. *Z. Naturforsch* **1978**, *33A*, 610.

(13) Lerner, R. G.; Dailey, B. P.; Friend, J. P. *J. Chem. Phys.* **1957**, *26*, 680.

(14) Miyazawa, T. *Bull. Chem. Soc. Jpn.* **1961**, *34*, 691.

(15) Miyazawa, T.; Pitzer, K. S. *J. Chem. Phys.* **1959**, *30*, 1076.

(16) Bernitt, D. L.; Hartman, K. O.; Hisatsune, I. *C. J. Chem. Phys.* **1965**, *42*, 3553.

(17) Bertie, J. E.; Michaelian, K. H. *J. Chem. Phys.* **1982**, *76*, 886.

(18) Bertagnolli, H.; Chieux, P.; Hertz, H. G. *Ber. Bunsen-Ges. Phys. Chem.* **1984**, *88*, 977.

(19) (a) Ruschin, S.; Bauer, S. H. *J. Phys. Chem.* **1980**, *84*, 3066. (b) Blom, C. E.; Gunthard, H. H. *Chem. Phys. Lett.* **1981**, *84*, 267.

(9) Jorgensen, W. L.; Ibrahim, M. J. *Am. Chem. Soc.* **1981**, *103*, 3976. Briggs, J. M.; Matsui, T.; Jorgensen, W. L. *J. Comput. Chem.* **1990**, *11*, 958.

TABLE II: Calculated Complexation Energies (kcal/mol) and Geometries^a

complex	OPLS			6-31G(d)		
	r_{OH}	θ	$-\Delta E$	r_{OH}	θ	$-\Delta E$
AcOH...HOH(I)	1.73	106	6.67	2.00	119	5.64
AcOH...HOH (II)	1.79	138	5.65	2.04	118	5.48
AcOH...HOH (III)	1.84	124	3.72	2.16	120	3.04
AcOH...HOH (IV)	1.82	139	3.47	2.19	142	2.44
AcOH...HOH (V)	1.68	121	8.76	1.86	112	8.65
(AcOH) ₂ (VI)	1.70	137, ^b 173 ^c	14.95			
AcOMe...HOH (I)	1.81	145	5.55	2.03	137	5.84
AcOMe...HOH (II)	1.81	144	4.98	2.04	121	5.54
AcOMe...HOH (III)	1.91	127	2.90	2.15	118	3.09
AcOMe...HOH (IV)	1.93	140	2.67	2.15	134	2.76

^a Lengths in angstroms, angles in degrees, and energies in kcal/mol. ^b $\angle C=O...H$. ^c $\angle O-H...O=$.

TABLE III: Energetic Results for the Liquids^a

liquid	$T, ^\circ C$	$-E_i(l)$	$E_{intra}(l)$	$E_{intra}(g)$	ΔH°_v	$\Delta H^\circ_v(exptl)$
acetic acid	25	12.41 ± 0.02	0.52 ± 0.003	0.31	12.79 ± 0.02	12.49^b
	100	11.31 ± 0.02	0.66 ± 0.003	0.40	11.80 ± 0.02	11.30^c
methyl acetate	25	7.36 ± 0.02	0.32 ± 0.002	0.31	7.95 ± 0.02	7.76^d

^a Energies and enthalpies in kcal/mol. ^b Wagman, D. D.; Evans, W. H.; Parker, V. B.; Schumm, R. H.; Halow, I.; Bailey, S. M.; Churney, K. L.; Nuttall, R. L. *J. Phys. Chem. Ref. Data, Suppl.* 2 **1982**, 11, 2-93. ^c Armitage, J. W.; Gray, P. *Trans. Faraday Soc.* **1962**, 58, 1746. ^d Svoboda, V.; Uchytlova, V.; Majer, V.; Pick, J. *Collect. Czech. Chem. Commun.* **1980**, 45, 3233.

and the E/Z energy differences are 4.98 and 2.67 kcal/mol. High-level ab initio calculations also predict barrier heights near 13 kcal/mol for both compounds; however, the E/Z energy difference is now greater for the ester (8.6 kcal/mol) than the acid (5.9 kcal/mol).²⁰ The populations of the E conformers are clearly low under normal conditions, which leads to difficulties for their detection. For the present purposes, the same Fourier coefficients were used for acetic acid and methyl acetate since, overall, the barrier heights and E/Z differences seem similar. The coefficients that give the best fit to the MM2 data for acetic acid are $V_1 = 4.98$ kcal/mol and $V_2 = 6.20$ kcal/mol. These assignments result in a barrier height of 8.94 kcal/mol and an E/Z energy difference of 4.98 kcal/mol. In the simulations, the monomers were initially all in the Z form and they predominately remained in that torsional well.

Results and Discussion

Bimolecular Complexes. Intermolecular geometry optimizations were performed for bimolecular complexes of acetic acid and methyl acetate with a water molecule as summarized in Figure 1 and Table II. Four monohydrated complexes were studied for both compounds (I-IV). Two additional complexes were investigated for acetic acid, namely, the linear hydrogen-bonded complex (V) and the cyclic dimer (VI). Interaction energies and geometries were computed for complexes I-V from ab initio molecular orbital calculations using the 6-31G(d) basis set.²¹ Calculations at this level have been found previously to provide excellent descriptions of hydrogen bonding.²² The intermolecular geometry optimizations were performed with both monomers fixed in their experimental geometries.²¹ The same approach was used for geometry optimizations of complexes I-VI using the OPLS potentials including the TIP4P model for water.²

Results in Table II from the OPLS calculations are found to mirror the trends from the 6-31G(d) optimizations. For both acetic acid and methyl acetate, the orderings of the interaction energies with water are in accord. The quantitative agreement is also reasonable, though exact accord was not sought in the fitting. The strongest interaction is for the complex V with acetic

TABLE IV: Volumes and Densities for the Liquids^a

liquid	$T, ^\circ C$	V	$V(exptl)$	d	$d(exptl)$
acetic acid	25	95.8 ± 0.2	95.5^b	1.041 ± 0.002	1.044^b
	100	102.6 ± 0.3	104.1^b	0.972 ± 0.003	0.958^b
methyl acetate	25	135.9 ± 0.3	132.7^c	0.905 ± 0.002	0.927^c

^a Volumes in \AA^3 and densities in g/cm^3 . ^b Hales, J. L.; Gundry, H. A.; Ellender, J. H. *J. Chem. Thermodyn.* **1983**, 15, 211. ^c Timmermans, J. *Physico-Chemical Constants of Pure Organic Compounds*; Elsevier: Amsterdam, 1950.

acid as the hydrogen-bond donor, followed by structures I and II in which the carbonyl oxygen is the acceptor.

It should be noted that the intermolecular distances predicted by the OPLS parameters are consistently shorter than those from the ab initio calculations by ca. 0.2 \AA . This is typical of the OPLS two-body potentials for hydrogen-bonded systems.²⁵ The inclusion of variable polarization is undoubtedly needed to simultaneously fit results for gas-phase complexes and pure hydrogen-bonded liquids.

For the cyclic acetic acid dimer, the predicted dimerization energy is -14.95 kcal/mol, which compares well with experimental values of $-14.6 \pm 0.5^{23a,b}$ and -14.92 kcal/mol.^{23c} In a previous study of amides, the cyclic dimerization energy for formamide was computed to be -14.07 kcal/mol,^{5b} and an experimental value for formic acid is -14.8 kcal/mol.^{23a}

In summary, the present OPLS parameters provide a reasonable description of the gas-phase bimolecular complexes. However, Monte Carlo simulations for the pure liquids were the key tests in attempting to fit, in particular, the experimental densities and heats of vaporization. The results of these simulations are given in the sections that follow.

Thermodynamics. The thermodynamic results from the three liquid simulations are summarized in Tables III-V. The uncertainties ($\pm 1\sigma$) for the computed quantities were obtained from separate averages over batches of 50 K or 100 K configurations. The total energy of the liquid is defined as the sum of the intermolecular, $E_i(l)$, and the intramolecular, $E_{intra}(l)$, energies. The heat of vaporization to the ideal gas, ΔH°_v , is then given by eq 3, where $E_{intra}(g)$ is computed from Boltzmann distributions

$$\Delta H^\circ_v = E_{intra}(g) - (E_i(l) + E_{intra}(l)) + RT \quad (3)$$

for eq 2. The heat capacity, $C_p(l)$, is computed from fluctuations

- (20) Wiberg, K. B.; Laidig, K. E. *J. Am. Chem. Soc.* **1987**, 109, 5935.
 (21) Hariharan, P. C.; Pople, J. A. *Theor. Chim. Acta* **1973**, 28, 203.
 Frisch, M. J.; Binkley, J. S.; Schlegel, H. B.; Raghavachari, K.; Melius, C. F.; Martin, R. L.; Stewart, J. J. P.; Bobrowicz, F. W.; Rohlfing, C. M.; Kahn, L. R.; DeFrees, D. J.; Seeger, R.; Whiteside, R. A.; Fox, D. J.; Fleuder, E. M.; Pople, J. A. *GAUSSIAN 86*; Carnegie-Mellon Quantum Chemistry Publishing Unit: Pittsburgh, 1984.
 (22) Dill, J. D.; Allen, L. C.; Topp, W. C.; Pople, J. A. *J. Am. Chem. Soc.* **1975**, 97, 7220.

- (23) (a) Claque, A. D. H.; Bernstein, H. J. *Spectrochim. Acta* **1969**, 25A, 593. (b) Chao, J.; Zwolinski, B. J. *J. Phys. Chem. Ref. Data* **1976**, 7, 363. (c) Furup, D. J.; Curtiss, L. A.; Blander, M. *J. Am. Chem. Soc.* **1980**, 102, 2610.

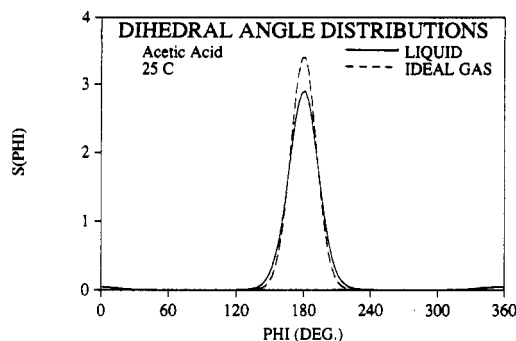


Figure 2. Dihedral angle distributions for acetic acid at 25 °C. Units are mole percent per degree for $S(\phi)$ in Figures 2 and 3.

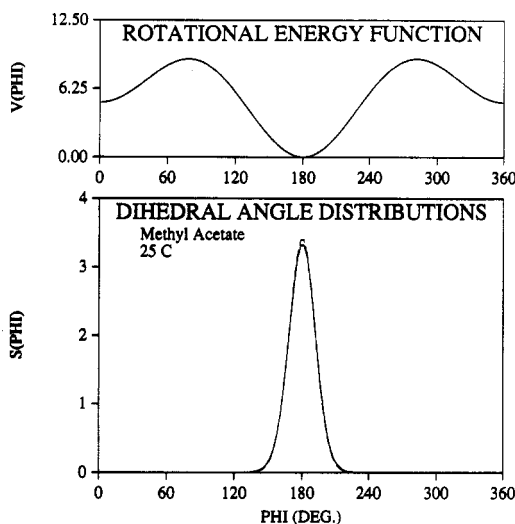


Figure 3. Rotational energy function and dihedral angle distributions for methyl acetate at 25 °C. The dashed line represents the gas-phase results and the solid line is computed for the liquid. Units are kcal/mol for $V(\phi)$.

in the enthalpy plus an intramolecular term, which is taken as the heat capacity of the ideal gas, $C_p(\text{ig})$, less R .³ The isothermal compressibility, κ , is computed from fluctuations in the volume, and the coefficient of thermal expansion, α , is obtained from fluctuations in the volume and enthalpy. It is known, however, that κ and α converge slowly and have large uncertainties, while the energies and volume converge relatively rapidly.²⁴ In Table III, the computed heats of vaporization are within 2.5% of the experimental values at 25 °C, while the error is 4.5% for acetic acid at 100 °C. The computed densities given in Table IV for acetic acid are within ca. 1% of the experimental values, while the error for methyl acetate is 2.5%. The calculated heat capacities (Table V) also agree well with the experimental data. While the computed compressibilities and expansivities have the right order of magnitude, their convergence is questionable. The computed expansivity of acetic acid at 25 °C of $(77 \pm 10) \times 10^{-5} \text{ K}^{-1}$ is lower than the experimental value of $108 \times 10^{-5} \text{ K}^{-1}$.⁸ The computed isothermal compressibility (κ) for acetic acid at 25 °C is also lower than experiment $((61 \pm 7) \times 10^{-6} \text{ vs } 93 \times 10^{-6} \text{ atm}^{-1})$.⁸

Conformational Equilibria. The computed *E/Z* conformer populations are given in Table VI, and plots of the dihedral angle distributions for the gas and liquid are shown in Figures 2 and 3. The gas-phase distributions were computed from Boltzmann distributions of eq 2. It should be recalled that all of the molecules were started in the *Z* form. There appears to be a small condensed-phase effect on the dihedral angle distribution for acetic acid at 25 °C (Figure 2). The distribution of dihedral angles broadens for the *Z* conformer on going from the gas to the liquid and 2% of the molecules converted to the *E* form. At 100 °C this value increased to 3%. The 2–3% traversal of the 8.9 kcal/mol barrier is notable particularly since umbrella sampling was not

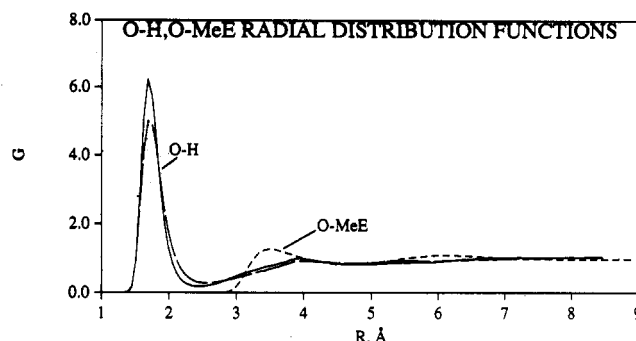


Figure 4. O-H and O-MeE radial distribution functions for acetic acid at 25 (solid) and 100 °C (long dashes) and methyl acetate at 25 °C (short dashes). O is the carbonyl oxygen, and MeE is the ester methyl group. Distances are in angstroms throughout.

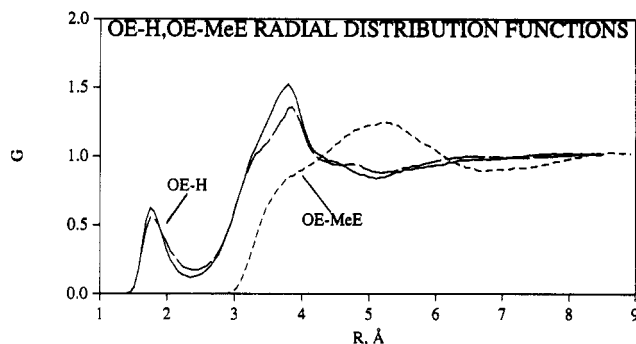


Figure 5. OE-H and OE-MeE radial distribution functions for acetic acid and methyl acetate. OE is the hydroxyl/ester oxygen. Correspondences are as in Figure 4 throughout.

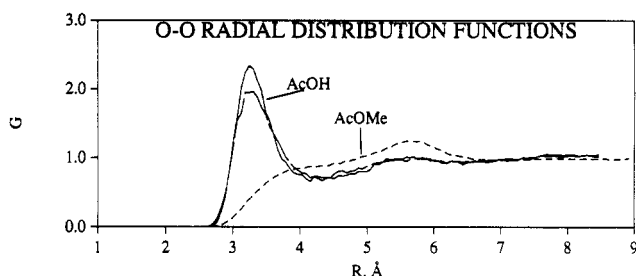


Figure 6. O-O radial distribution functions for acetic acid and methyl acetate.

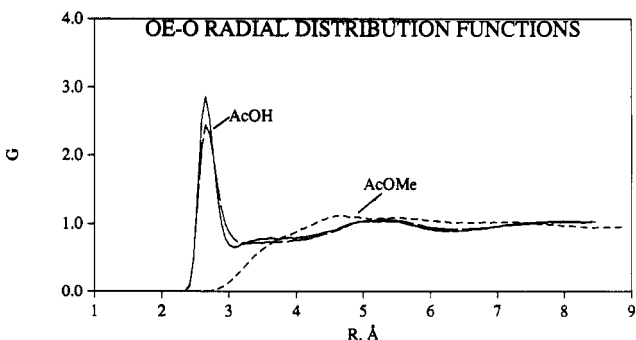


Figure 7. OE-O radial distribution functions for acetic acid and methyl acetate.

employed, which could have facilitated the transition. Though lengthy sampling was carried out, it is not clear that the *E* and *Z* populations have converged in view of the barrier height. Nevertheless, a condensed-phase effect in the computed direction would be reasonable in view of the polarity of the medium and the enhanced dipole moment for the *E* form (5.1 D) versus the *Z* form (1.5 D) based on the OPLS charges.

The dihedral angle distributions for methyl acetate at 25 °C are unimodal with a narrow peak for the *Z* well (Figure 3). A

TABLE V: Heat Capacities, Expansivities, and Compressibilities of the Liquids^a

liquid	T, °C	C _p (ig)	C _p (l)	C _p (l) ^{exptl}	10 ³ α	10 ⁶ κ
acetic acid	25	15.9 ^b	26.06 ± 1.0	29.7 ^b	77 ± 10	61 ± 7
	100	18.0 ^c	30.95 ± 1.4	33.0 ^d	88 ± 11	81 ± 8
methyl acetate	25	20.6 ^e	30.25 ± 1.2	29.54 ^f	111 ± 13	87 ± 9

^a C_p in cal/mol deg; α in deg⁻¹; κ in atm⁻¹. ^b Wagman, D. D.; Evans, W. H.; Parker, V. B.; Schumm, R. H.; Halow, I.; Bailey, S. M.; Churney, K. L.; Nuttall, R. L. *J. Phys. Chem. Ref. Data Suppl.* **2** 1982, 11, 2-93. ^c Reference 23b. ^d Armitage, J. W.; Grew, P. *Trans. Faraday Soc.* **1962**, 58, 1746. ^e Chao, J.; Hall, K. R.; March, K. N.; Wilhoit, R. C. *J. Phys. Chem. Ref. Data* **1986**, 15, 1369. ^f Hall, Jr., H. K.; Baldt, J. H. *J. Am. Chem. Soc.* **1971**, 93, 140.

TABLE VI: Calculated Conformer Populations

compd	T, °C	conformation	% gas ^a	% liquid ^b
acetic acid	25	Z	100.0	97.9 ± 0.08
		E	0.0	2.1 ± 0.06
	100	Z	99.8	96.8 ± 0.02
		E	0.2	3.2 ± 0.08
methyl acetate	25	Z	100.0	100.0 ± 0.0
		E	0.0	0.0 ± 0.0

^a Calculated from a Boltzmann distribution. ^b Results from the Monte Carlo simulations.

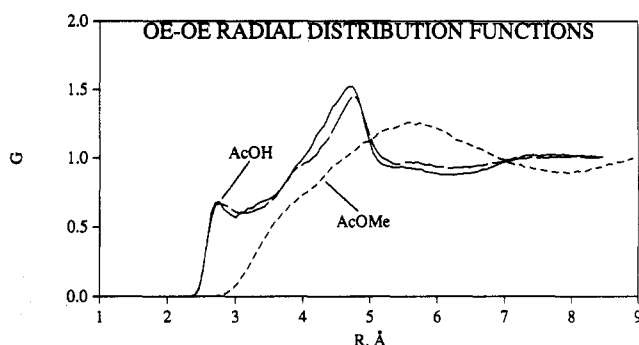


Figure 8. OE-OE radial distribution functions for acetic acid and methyl acetate.

condensed-phase effect on the dihedral angle populations is not evident in this case. Although the dielectric constant for methyl acetate (6.68)¹⁰ is nearly identical with that for acetic acid and although the dipole moment increases from 1.44 to 4.18 D on going from Z- to E-methyl acetate, no E conformers were generated during the simulation. This may be due to the shorter duration of the simulation or the absence of the hydrogen-bonding interactions. A plot of the $V(\Phi)$ used for both acetic acid and methyl acetate is given at the top of Figure 3.

Radial Distribution Functions. Five of the computed atom-atom radial distribution functions (rdfs) for acetic acid and methyl acetate are given in Figures 4-8. In these Figures O is the carbonyl oxygen, OE is the hydroxyl or ester oxygen, and MeE is the alkoxy methyl group in the ester. All data given in this section for acetic acid apply to both 25 and 100 °C unless otherwise indicated. The results for acetic acid at both temperatures are similar with the expected reduction in structure at the higher temperature due to increased population of higher energy configurations. Hydrogen-bonding interactions are clearly indicated by the strong first peak in the O-H rdfs (Figure 4). The maximum is at 1.7 Å. Integration out to the minimum at 2.4 Å for 25 °C yields 0.88 contacts or ca. 1.76 hydrogen-bonding interactions of this type per molecule, while integration to 2.6 Å for 100 °C produces 1.74 hydrogen bonds. The corresponding O-MeE rdf (Figure 4) for methyl acetate exhibits a weak maximum at 3.5 Å. Integration out to the minimum at 4.8 Å yields 2.5 contacts.

In contrast to the O-H rdfs, the OE-H rdfs in Figure 5 exhibit a weak peak at 1.8 Å, which when integrated out to 2.4 Å yields only 0.25 neighbors. It is clear that the majority of the hydrogen-bonding interactions occur with the carbonyl and not the hydroxyl oxygen and that each molecule is participating in an average of two hydrogen bonds, one as donor and one as acceptor. The preference for hydrogen bonding with the carbonyl oxygen is fully consistent with the results for the bimolecular complexes with water in Table II. The stronger second peak at 3.8 Å (3.9

Å for 100 °C) in the OE-H rdfs is also notable and can be assigned to the hydrogens that are hydrogen-bonded to the carbonyl oxygen of the reference molecule containing OE. In comparison, the OE-MeE rdf for methyl acetate is broad and relatively featureless.

The three oxygen-oxygen rdfs are given in Figures 6-8. For acetic acid, the O-O and OE-O rdfs both have strong first peaks; the maximum for the O-O rdf occurs at 3.3 Å, and that for the OE-O rdf is at 2.7 Å. Integration out to the first minimum in the O-O rdf at 4.2 Å yields 2.8 and 2.5 contacts for 25 and 100 °C. The integral of the OE-O rdfs for acetic acid out to 3.1 and 3.2 Å yields 0.96 and 1.00 contacts at 25 and 100 °C. These peaks reflect the ca. 2 OE-O hydrogen bonds for each monomer. The broad hump at ca. 5.2 Å corresponds to the pair of oxygens in the reference dimer that are not involved in the hydrogen bonding.

The OE-OE rdfs for acetic acid exhibit maxima at 2.8 and 4.8 Å with a shoulder at ca. 4.0 Å. These features can be rationalized by the presence of three general types of acetic acid dimers, namely, those that correspond to structures I and II, where H₂O is replaced with AcOH, and VI in Figure 1. For comparison, the distances between the oxygen in water and the hydroxyl oxygen in acetic acid in structures I and II are 3.1 and 5.0 Å. In addition, the shoulder at ca. 4.0 Å in the OE-OE rdf corresponds well with the OE-OE distance in structure VI which is 3.9 Å.

Hydrogen-Bonding Analyses. Hydrogen bonding at the carbonyl oxygen in acetic acid was analyzed from configurations saved every 10 K during the simulations. As a result, 250 configurations were considered at 25 and 100 °C. A hydrogen bond was defined to have an interaction that was stronger than -4.0 kcal/mol and by an $\text{O}\cdots\text{H}$ distance that was less than 2.41 Å at 25 °C and 2.59 Å at 100 °C. The two constraints were chosen to guarantee that the analyzed pairs were truly hydrogen bonded and not just proximal or interacting favorably in another fashion. The specific distance and energy criteria were based on the extent of the first peaks in the O-H rdfs and in the energy pair distribution function (vide infra). The occurrence of interactions of this strength at the hydroxyl oxygen is negligible, so only hydrogen bonds involving the carbonyl oxygen were considered.

A number of studies have appeared concerning the nature of the interaction between acetic acid molecules in condensed phases. It is clear that at low concentrations in non-hydrogen-bonding solvents, acetic acid is composed mainly of cyclic dimers.²⁵⁻²⁸ The nature of association in the pure liquid is less well established. Some results indicate that acetic acid consists mainly of cyclic dimers, while other studies suggest that the liquid is made up of polymers, dimers, and monomers in equilibrium. Elucidation of the structure of the liquid is complicated by the fact that even small amounts of impurity (ca. 3%) can significantly affect the results.²⁹

Raman spectra for acetic acid have been interpreted to indicate that cyclic dimers predominate with some chains, dimers, and monomers also present.²⁹⁻³² One low-frequency Raman study,

(25) Reeves, L. W.; Schneider, W. G. *Trans. Faraday Soc.* **1958**, 54, 314. Reeves, L. W. *Trans. Faraday Soc.* **1959**, 55, 1684.

(26) Reuben, J. *J. Am. Chem. Soc.* **1969**, 91, 5725.

(27) Bellamy, L. J.; Lake, R. F.; Pace, R. J. *Spectrochim. Acta* **1963**, 19, 443.

(28) Fujii, Y.; Yamada, H.; Mizuta, M. *J. Phys. Chem.* **1988**, 92, 6768.

(29) Nielsen, O. F.; Lund, P.-A. *J. Chem. Phys.* **1983**, 78, 652.

(30) Semmler, J.; Irish, D. E. *J. Solution Chem.* **1988**, 17, 805.

(31) Ng, J. B.; Shurvell, H. F. *Can. J. Spectrosc.* **1985**, 30, 149.

(32) Waldstein, P.; Blatz, L. A. *J. Phys. Chem.* **1967**, 71, 2271.

TABLE VII: Results of the Hydrogen-Bond Analyses for Liquid Acetic Acid^a

	25 °C	100 °C
no. of H-bonds	1.8	1.7
ϵ (H-bond)	-7.11	-7.07
ϵ (Coulomb)	-7.50	-7.36
ϵ (Lennard-Jones)	0.39	0.29
θ , deg	161	158
γ , deg	144	140

% Monomers in n H-Bonds		
n	25 °C	100 °C
0	1.3	3.5
1	25.4	36.4
2	64.1	52.0
3	8.8	7.6
4	0.3	0.4

^a ϵ 's in kcal/mol. ϵ (H-bond) is the average hydrogen bond energy that can be decomposed into Coulomb and Lennard-Jones terms. A hydrogen bond is defined by an interaction energy of -4.0 kcal/mol or less and an $\text{O}\cdots\text{H}$ separation less than 2.41 (25 °C) or 2.59 Å (100 °C). The angles θ and γ are $\angle\text{O}-\text{H}\cdots\text{O}=\text{}$ and $\angle\text{C}=\text{O}\cdots\text{H}$.

TABLE VIII: Results from the Cyclic Dimer Analysis of Liquid Acetic Acid^a

	25 °C	100 °C
% cyclic	7.3	11.8
av energy	-12.5	-12.3
highest energy	-5.7	-5.0
lowest energy	-15.1	-15.1
av $\text{O}\cdots\text{H}$ dist	1.85	1.86

^aEnergies in kcal/mol, distances in angstroms. The criteria for a cyclic dimer are that the $\text{O}\cdots\text{H}$ and $\text{H}\cdots\text{O}=\text{}$ distances for a pair of acetic acid molecules are both within 2.5 Å.

however, reassigned a band near 50 cm^{-1} that had been attributed to cyclic dimers²⁹ to the pseudo-lattice vibrations found in most liquids.³³ It was concluded that the liquid is not necessarily composed of cyclic dimers. ¹H NMR studies have suggested that liquid acetic acid is composed of cyclic dimers, trimers, tetramers, and linear polymers in equilibrium.^{25,26,34,35} An X-ray study of the liquid in 1965 led to an interpretation in terms mainly of cyclic dimers.³⁶ In 1973, however, this study was called into question, and new X-ray data for acetic acid indicated an equilibrium between rings and long chains.³⁷

An IR study in 1963 led to the claim that liquid acetic acid consists mainly of chains,²⁷ while another study in 1967 disputed this in favor of rings.³⁸ A neutron diffraction study of the liquid revealed that, while the data could be fit with hydrogen-bonded chains, a better model was the cyclic dimer.³⁹ Pure acetic acid and mixtures with acetone were also found to absorb an excess of ultrasound.⁴⁰ These data were interpreted to be consistent with an equilibrium between cyclic and open dimers. Most of the studies described above involved the initial assumption of a model. The parameters for this model were then optimized to best fit the data. Additionally, in many cases the cyclic dimer was the only model considered. To further investigate the average structure of liquid acetic acid, hydrogen-bonding and cyclic dimer analyses were performed on the present Monte Carlo results. The findings are summarized in Tables VII and VIII.

At 25 °C each acetic acid molecule was found to participate in, on average, 1.8 hydrogen bonds with an average energy of -7.11

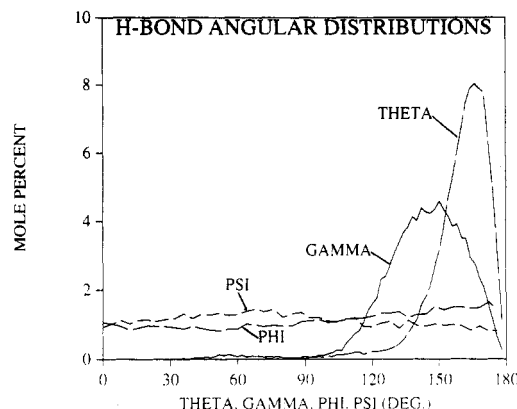


Figure 9. Distributions for hydrogen-bond angles in liquid acetic acid at 25 °C computed with the OPLS functions. γ , θ , ϕ , and ψ are the $\text{O}-\text{H}\cdots\text{O}=\text{}$, $\text{C}=\text{O}\cdots\text{H}$, $\text{C}=\text{O}\cdots\text{H}-\text{O}$, and $\text{O}-\text{C}=\text{O}\cdots\text{H}$ angles, respectively. Units on the ordinate are mole percent of hydrogen bonds per degree.

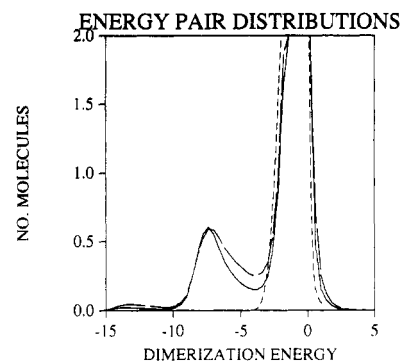


Figure 10. Distributions of the individual interaction energies (kcal/mol) between molecules in liquid acetic acid at 25 (solid) and 100 °C (long dashes) and methyl acetate at 25 °C (short dashes).

kcal/mol. At 100 °C these figures became 1.7 and -7.07 kcal/mol. These numbers correspond well with those obtained from integration of the first peak in the $\text{O}-\text{H}$ rdf, which amounted to 1.76 and 1.74 hydrogen bonds at 25 and 100 °C. There are very few non-hydrogen-bonded monomers present in the liquid, 1.3% at 25 °C and 3.5% at 100 °C. At 25 °C, 64% of the molecules are involved in two hydrogen bonds, while 9% are involved in three hydrogen bonds. At 100 °C, the proportion of polymers ($n \geq 2$) decreases and more monomers, dimers, and chain ends are present. Over half of the molecules are still involved in two or more hydrogen bonds at 100 °C. A plot of the hydrogen bond angular distributions is given in Figure 9. The $\angle\text{O}-\text{H}\cdots\text{O}=\text{}$ (θ) and $\angle\text{C}=\text{O}\cdots\text{H}$ (γ) angles at 25 °C have average values of 161° and 144°, while at 100 °C they flex more to averages of 158° and 140° (Table VIII). The distribution of γ 's is relatively broad, covering a range of ca. 100°, while the range for θ is narrower. The dihedral angles $\angle\text{C}=\text{O}\cdots\text{H}-\text{O}$ (ϕ) and $\angle\text{O}-\text{C}=\text{O}\cdots\text{H}$ (ψ) reveal no significant orientational preference for the pairs. If the liquid were composed predominately of planar cyclic dimers, the dihedral angle distributions for ϕ and ψ would both favor the region near 0°.

The computed energy pair distributions are shown in Figure 10. The distributions at 25 and 100 °C have the typical shape for hydrogen-bonded liquids with a spike near 0 kcal/mol, which represents the interactions with distant molecules in the bulk and a low-energy band for hydrogen-bonded neighbors.² Acetic acid also displays a second very low energy band centered near -13 kcal/mol at both 25 and 100 °C that can arise only from cyclic dimers. An analogous low-energy band was found in the previous study of liquid formamide.^{5b} It is clear, however, due to the small size of the peak, that the fraction of monomers in cyclic dimers is relatively small. An evaluation of the 250 saved configurations for cyclic dimers produced the data given in Table VIII. Cyclic dimers were defined as pairs with interaction energies below -4

(33) Bertie, J. E.; Michaelian, K. H. *J. Chem. Phys.* **1982**, *77*, 5267.

(34) Akitt, J. W. *J. Chem. Soc., Faraday Trans. 1* **1977**, 1622.

(35) Clark, J. H.; Emsley, J. *J. Chem. Soc., Dalton Trans.* **1973**, 2154.

(36) Gultvits, N. I.; Lutsikii, A. E.; Radchenko, I. V. *Zh. Strukt. Khim.* **1965**, *6*, 27.

(37) Gorbunova, T. V.; Shilov, V. V.; Batalin, G. I. *Zh. Strukt. Khim.* **1973**, *14*, 424.

(38) Jakobsen, R. J.; Mikawa, Y.; Brasch, J. W. *Spectrochim. Acta* **1967**, *23A*, 2199.

(39) Bertagnolli, H. *Chem. Phys. Lett.* **1982**, *93*, 287.

(40) Corsaro, R. D.; Atkinson, G. *J. Chem. Phys.* **1971**, *54*, 4090.

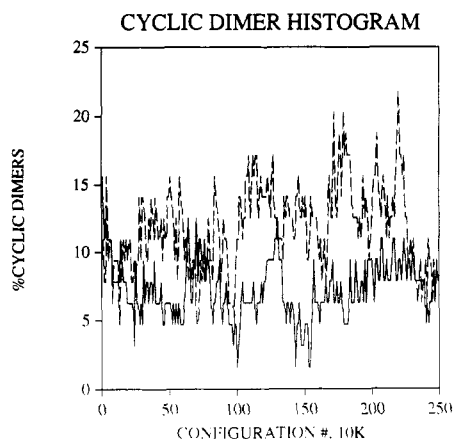


Figure 11. Histogram of the percentage of monomers that are in cyclic dimers per configuration analyzed for acetic acid at 25 (solid) and 100 °C (dashed).

kcal/mol and that had $\text{=O1}\cdots\text{H2}$ and $\text{=O2}\cdots\text{H1}$ distances that were both within 2.5 Å. While many of the dimers were relatively planar, some were significantly bent and occasionally stacked.

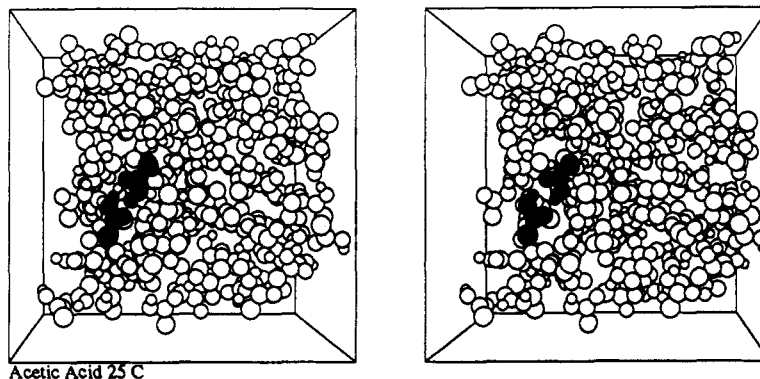


Figure 12. Stereoplot of the last configuration from the Monte Carlo simulation of acetic acid at 25 °C. The darkened pair of molecules illustrate a cyclic dimer. The radii of the balls have been chosen for visual comfort and are in the order $\text{Me} > \text{C} > \text{O} > \text{H}$.

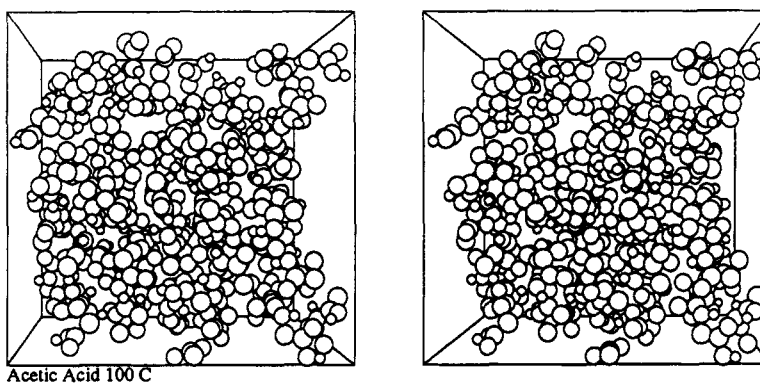


Figure 13. Stereoplot of the last configuration from the Monte Carlo simulation of acetic acid at 100 °C.

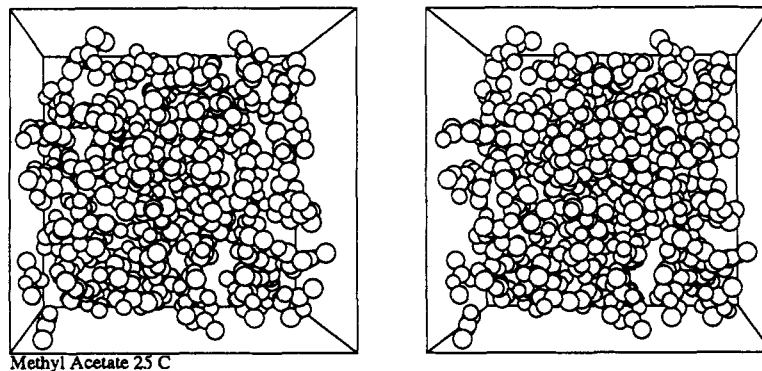


Figure 14. Stereoplot of the last configuration from the Monte Carlo simulation of methyl acetate at 25 °C.

Interestingly, at 25 °C only 7% of the monomers were in cyclic dimers, while at 100 °C the percentage increased to 12%. This undoubtedly accompanies a reduction in longer chain polymers. Convergence of the population of cyclic dimers was a concern in view of the cohesiveness of the liquid. As a consequence, the simulations were equilibrated for 6000 K instead of the usual 500–1000 K. In addition, averaging and subsequent analysis were performed for 250 saved configurations obtained from a 2500 K averaging run. The fluctuation in the percentage of monomers involved in cyclic dimers was monitored and was found to vary from 2 to 16% at 25 °C and from 5 to 22% at 100 °C (Figure 11). It is clear from Figure 11 that the fluctuations over the analyzed configurations were quite significant and that there was no pronounced drift. The percentage of monomers involved in cyclic dimers fluctuated upward somewhat at 100 °C until ca. 2300 K, when it then dramatically decreased.

Finally, two additional simulations were performed to investigate the cyclic dimer issue. In the first, a configuration was selected from the simulation at 100 °C that had the highest cyclic dimer content (22%). This configuration was cooled to 25 °C, equilibrated for 500 K, and averaged for 2500 K. Although the simulation started out with 22% of the monomers involved in cyclic dimers, the percentage quickly dropped off to ca. 9% for the first

half of the simulation (ca. 1200 K) but then averaged ca. 16%. In the final simulation, the liquid was initially composed entirely of cyclic dimers. This was accomplished by generating cyclic dimers with the geometrical parameters obtained from the OPLS optimization of the cyclic dimer (VI in Figure 1). They were mapped onto a fully equilibrated cube of liquid 12-site benzene.⁴¹ As in the previous simulations, all of the monomers were permitted to move independently. The simulation was run for 500 K configurations of equilibration and averaged for 2500 K. The percentage of monomers involved in cyclic dimers decreased during the equilibration phase so that it was only 50% at the beginning of averaging. The cyclic dimer content slowly decreased during the first half of the averaging phase and hovered around 15% for the remainder of the simulation. These results clearly indicate that the liquid prefers open dimers and hydrogen-bonded chains to the cyclic dimers, and the percentage of monomers in cyclic dimers at 25 °C is no more than ca. 15% from these simulations.

Stereoplots of the final configurations from the simulations are given in Figures 12-14. The periodicity of the cell must be remembered when viewing, such that a molecule that is near one face of the cube is also near the molecules at the opposite face. Also, the illustrated box edges are outside the edges of the actual periodic cube. Long hydrogen-bonded chains can be seen in the plots of acetic acid along with some cyclic dimers. The darkened

pair in Figure 12 represents one such cyclic dimer. The stereoplot of methyl acetate confirms the lack of any obvious organized structure, which is reflected in the relatively featureless rdfs.

Conclusion

Potential functions in the OPLS format have been developed and tested for liquid acetic acid and methyl acetate. The functions have been shown to reproduce heats of vaporization within 2-4% and densities within 2% of experimental data. The structural results for liquid acetic acid are reasonable for a strongly hydrogen-bonded liquid. Most of the liquid is composed of hydrogen-bonded chains; however, a small percentage (ca. 7-12%) of monomers are in cyclic dimers. Since there is no general accord among the experimental studies on the structure of the liquid, the present results support some of the earlier work but are at variance with the studies that claim that the liquid is predominately composed of cyclic dimers. Indirect support for the present predictions comes from the fact that the current model reproduces well the experimentally determined dimerization energy along with thermodynamic properties of the liquid. In addition, the current parameters have been successfully used in other recent studies.^{4,5,7}

Acknowledgment. Gratitude is expressed to Daniel L. Severance for computational assistance and to the National Science Foundation and the National Institutes of Health for support of this work.

Registry No. Acetic acid, 64-19-7; methyl acetate, 79-20-9.

(41) Jorgensen, W. L.; Severance, D. L. *J. Am. Chem. Soc.* **1990**, *112*, 4768.

Heat Capacities of Some Primary Alcohols in Dodecyltrimethylammonium Bromide Aqueous Solutions

R. De Lisi,* S. Milioto,

Department of Physical Chemistry, University of Palermo, via Archirafi 26, 90123 Palermo, Italy

and A. Inglese

Department of Chemistry, University of Bari, via Amendola 173, 70126 Bari, Italy (Received: May 21, 1990)

Heat capacities of the ternary systems water-dodecyltrimethylammonium bromide (DTAB)-alcohols (propanol, butanol, pentanol, hexanol, and heptanol) were measured at 25 °C as a function of the surfactant and the additive concentration. At fixed low surfactant concentrations m_S , the apparent molar heat capacity of alcohols $C_{\phi,R}$ increases linearly with alcohol concentration m_R , whereas at higher m_S , the sign of the slope of $C_{\phi,R}$ vs m_R changes from positive to negative at a m_R value that, regardless of the surfactant concentration, depends on the alcohol alkyl chain length. The longer the alcohol chain, the smaller the m_R value at which this occurs. Microheterogeneity formation by the alcohol can account for this behavior. From the least-squares analysis at low alcohol concentrations the standard partial molar heat capacities C_p° of propanol and hexanol in micellar solutions have been obtained as a function of m_S . The plot of C_p° vs m_S for hexanol displays a maximum of about 30 J K⁻¹ mol⁻¹ at ca. 0.3 mol kg⁻¹ DTAB; according to the literature, it can be ascribed to the DTAB postmicellar transition. In the case of propanol the maximum was not detected. The standard partial molar heat capacities of propanol and hexanol in micellar solutions in the region above the cmc and below the structural transition were rationalized in terms of the alcohol properties in the aqueous and micellar phases and the alcohol distribution between the two phases by using a previously reported equation, expanded to account for the temperature effect on the change of the mole fraction of alcohol solubilized in both phases. Previously, this effect was considered to be negligible. The same equation was also used to analyze the heat capacity data of butanol and pentanol already published. An important result obtained is that the standard heat capacity of alcohol in the micellar phase increases with the length of the alcohol alkyl chain. This effect was not previously observed when the temperature effect on the alcohol distribution was neglected.

Introduction

The standard partial molar properties of a solute Y° reflect both the intrinsic properties and the contribution of the interactions with its environment. Consequently, the profile of Y° as a function of the composition of a mixed solvent depends on the solute-solvent interactions. Special attention must be paid to the standard partial molar heat capacity since this property, which reflects the energy fluctuations, is the thermodynamic property most sensitive to the

structural changes occurring in the mixed solvent when its composition is varied.

It has been observed that the standard partial molar heat capacity of a hydrophobic solute in micellar solutions, C_p° , provides evidence of the existence of structural transitions of micelles.¹⁻³

(1) Quirion, F.; Desnoyers, J. E. *J. Colloid Interface Sci.* **1986**, *112*, 565.
(2) De Lisi, R.; Milioto, S. *J. Solution Chem.* **1987**, *16*, 767.